An STM and Monte Carlo study of the AlF_3 thin film growth on Cu(1 1 1)

2015 J. Phys. D: Appl. Phys. 48 265305

(http://iopscience.iop.org/0022-3727/48/26/265305)

IOP Publishing Journal of Physics D: Applied Physics
J. Phys. D: Appl. Phys. **48** (2015) 265305 (8pp) doi:10.1088/0022-3727/48/26/265305

An STM and Monte Carlo study of the AlF_3 thin film growth on Cu(1 1 1)

A E Candia[1], L Gómez[2], R A Vidal[1,3], J Ferrón [1,4] and M C G Passeggi Jr[1,4]

[1] Laboratorio de Física de Superficies e Interfaces, Instituto de Física del Litoral (CONICET-UNL), Güemes 3450, (3000) Santa Fe, Argentina
[2] FCEIA e Instituto de Física de Rosario, Universidad Nacional de Rosario, CONICET, Avda. Pellegrini 250, (2000) Rosario, Argentina
[3] Departamento de Física, Facultad de Ingeniería Química, Universidad Nacional del Litoral, Santiago del Estero 2829, (3000) Santa Fe, Argentina
[4] Departamento de Materiales, Facultad de Ingeniería Química, Universidad Nacional del Litoral, Santiago del Estero 2829, (3000) Santa Fe, Argentina

E-mail: adrianaecandia@gmail.com

Received 2 December 2014, revised 22 April 2015
Accepted for publication 5 May 2015
Published 3 June 2015

Abstract

We report measurements of AlF_3 thin film growth on Cu(1 1 1) at room temperature by means of scanning tunneling microscopy. The growth proceeds by the formation of fractal islands characterized by a very corrugated surface. Through uncovered zones and island density we determined a diffusion length of ~25 nm for the adsorbed molecules. Even with this large diffusion length the step-edges do not appear fully decorated. These experimental results are contrasted with simulations based on a limited diffusion aggregation model and Metropolis Monte Carlo.

Additionally, the results of the AlF_3 sub-monolayer growth on Cu(1 1 1) are compared with our previous results on Cu(1 0 0), finding that both systems show more differences than similarities. Thus, while the growth on Cu(1 0 0) shows fully decorated step-edges, on Cu(1 1 1), they present non-covered zones even at coverages as high as 0.7 monolayers. Supported on MC simulations we suggest that the qualitative difference between both faces is due to different step-edge behaviour.

Keywords: aluminium fluoride, copper, films growth, insulator-on-metal interfaces, scanning tunnelling microscopy, Monte Carlo method, diffusion

(Some figures may appear in colour only in the online journal)

1. Introduction

The composition, growth mechanism and structure of insulator thin films deposited on several metal surfaces have been the subject of extensive studies in the last years. The driving forces for such interest are the quality requirements of the thin films needed to develop advanced microelectronic, optical, and magnetic devices, as well as nanometer scale structures [1]. Lately there is growing interest in the use of thin insulating layers grown over metallic surfaces, e.g. to support nanostructures and decouple their electronic states from those of the substrate and reduce charging effects [2], to study the interaction between spins in linear chains of Mn atoms on CuN islands [3], or to assemble organic molecules [4], among other examples.

Some important efforts based on scanning tunnelling microscopy (STM) have been made in the last two decades in order to understand the growth of insulators on metals. Some years ago, Calleja *et al* [5] showed the epitaxial growth of CaF_2 on Cu(1 1 1) as a function of deposition temperature and coverage, reporting from their observations the epitaxial growth of twinned CaF_2(1 1 1) crystallites on Cu(1 1 1). Farías *et al* [6] found that the upper and lower sides of the step-edges act as nucleation centers during the growth of LiF molecules

on Ag(1 1 1), at a low temperature (77 K), suggesting that this nucleation mechanism should be present as well in other insulator-on-metal growth systems at low temperatures. On the other hand, Bertrams and Neddermeyer [7] reported the growth of NiO(1 0 0) layers on Ag(1 0 0), studying the coverage and sample heating effects during and following Ni deposition using STM and low-energy electron diffraction (LEED), and Fölsch *et al* [8] showed selective NaCl growth on Cu(2 1 1), where alternative stripes of bare Cu and NaCl covered areas were observed.

Insulator layers of aluminium fluoride (AlF_3) are of particular interest due to their potential application in nanometer scale patterning using electron beam lithography [9–14]. It is a well-known fact that under electron irradiation AlF_3 thin films show radiolysis, i.e. the desorption of fluoride with the consequent formation of an aluminium metallic layer [14–17]. Sánchez *et al* [18], reported a layer-by-layer (LbL) growth of AlF_3 thin films on Al(1 1 1) surfaces by means of Auger electron (AES) and electron energy loss (EELS) spectroscopies. Vergara *et al* [13], characterized the growth process of AlF_3 films on GaAs(1 1 0) from sub-monolayer coverages up to several layers, by means of AES, ion sputtering depth-profiling and direct recoiling spectroscopy with time of flight analysis (TOF-DRS), and in a latter work they studied the changes in the chemical structure of AlF_3 films by electron irradiation using AES and factor analysis (FA) [14].

Recently, we characterized the growth process of AlF_3 thin films on Cu(1 0 0) at room temperature by means of STM [19, 20]. We have shown that at the initial growth stages the AlF_3 molecules completely decorate both sides of the substrate step-edges. Then, islands are formed on the Cu terraces, increasing their size upon further evaporation, and displaying a shape evolution from a compact to a fractal-like form by clustering of islands of critical size $Ac \sim 2.5$ nm [19]. Although the islands never coalesce, they grow in a lateral 2D film covering the substrate with a single monolayer until ~0.8 monolayers (MLs), changing with further deposition to a 3D island growth mode. For this system we also described a new diffusion mechanism, in which the isotropic characteristic of the random movement of the AlF_3 molecules adsorbed over the surface is broken, in such a way that movement along certain directions is favoured [21]. This is due to the formation of bi-molecules (Al_2F_6) which break the system symmetry modifying the diffusion regime over the surface. The minimum energy state of a formed bi-molecule is reached when their Al–Al axis bends 60° over the surface, and aligns along the [1 1 0] axis of the FCC Cu lattice. This breakdown symmetry, with an almost free form of the reconstructed bi-molecule over the surface, transforms one symmetry direction of the Cu(1 0 0) surface as preferential. On the other hand, the tilted bi-molecule axis, and the competition between molecule–molecule and molecule-substrate interactions, makes not only a crystal axis as privileged, but also one of the movement directions. These movement channels produce an important change in the diffusion length and on the growth mode [21].

In this work, we characterize the AlF_3 thin film growth on Cu(1 1 1) by means of STM, and simulations based on a limited diffusion aggregation model (LDA-MC) and Metropolis Monte Carlo (MMC) calculations to understand the growth characteristic features based on kinetic and geometric factors. We also compare these results with previous ones obtained on Cu(1 0 0).

2. Experimental setup and simulations

2.1. Experimental conditions

The STM measurements were done at room temperature in an ultra-high vacuum (UHV) chamber with a base pressure in the low 10^{-10} mbar range. The Cu(1 1 1) substrate was cleaned in a secondary UHV chamber attached to the main one, by cycles of Ar^+ ion bombardment and annealing at 900 K. A chromel–alumel thermocouple, attached to the backside of the sample holder, was used to measure the sample temperature. The aluminium fluoride films were deposited at room temperature (300 K) onto the Cu(1 1 1) surface in the secondary chamber from a Knudsen cell, charged with anhydrous AlF_3 (CERAC INC., Milwaukee, Wisconsin, USA, 99.5%) and heated at 820 K. The cell was carefully degassed and shuttered to avoid sample contamination. Vacuum conditions in the secondary chamber were in the 10^{-9} mbar range, even during the evaporation. STM images of the clean Cu(1 1 1) substrate and AlF_3/Cu(1 1 1) samples showed no evidence of contamination even after maintaining them during several hours in the secondary chamber. Nevertheless, the samples were introduced into the UHV main chamber immediately after the preparation. The deposition rate of AlF_3 was varied between 6×10^{-3} and 2×10^{-2} ML s^{-1}. Its calibration and the reported coverages were determined from a direct analysis of the STM images.

Electrochemical etched tungsten tips were used for all STM experiments reported in this work. The polycrystalline W tips were routinely cleaned by Ar^+ ion bombardment in UHV. All the STM images obtained in this study were acquired in the constant current mode with relatively high positive sample bias voltages, between +2.20–2.50 V, i.e. injecting electrons in the conduction band of AlF_3, which indicates the insulating character of the film. The only exception was for atomic resolution images. For sample bias voltages lower than +2.20 V the islands are frequently swept away by the tip during the scanning, showing typical STM images of a '*clean*' Cu(1 1 1) surface, suggesting that AlF_3 molecules are adsorbed over the surface without a chemical reaction with copper atoms. The tunnelling currents used were in the range between 0.1–0.3 nA. Acquisition and image processing were performed using the WS × M free software [22].

2.2. Simulation methods

Two different MC [23] approaches were used along this work. One of them is based on realistic potentials, and was done with the aim of identifying the different mechanisms involved in the surface diffusion. The other one is based in the limited diffusion aggregation method, and was used to investigate possible geometric or shadowing effects, not involving any physical parameters. In the following we describe both approaches in more detail.

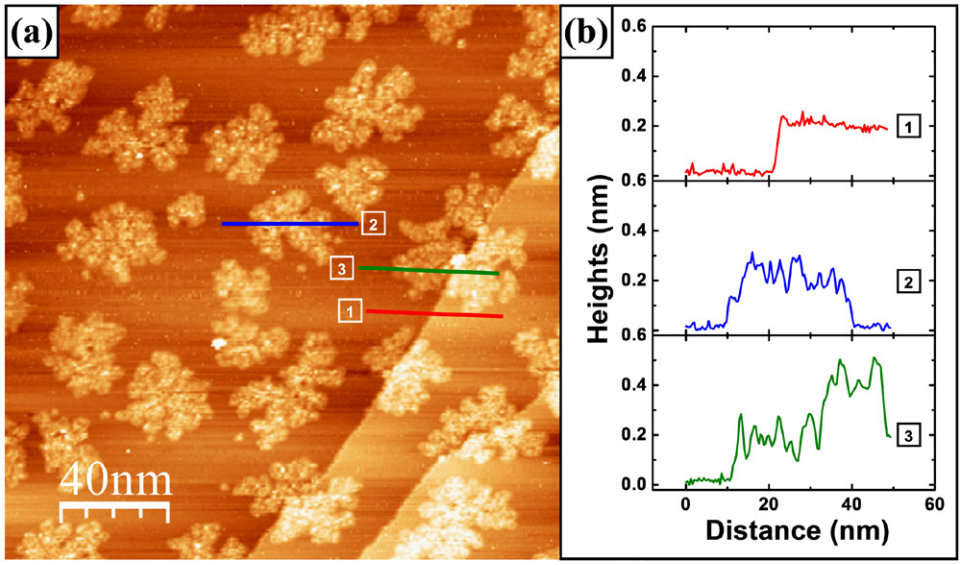

Figure 1. (a) STM image (200 nm × 200 nm) recorded after the deposition of 0.40 ML of AlF_3 on Cu(1 1 1); (b) apparent height profiles acquired along the lines depicted in (a). Heights of (1) a monoatomic Cu(1 1 1) clean step-edge, (2) an AlF_3 island on a terrace, and (3) AlF_3 islands grown at both sides of a step-edge, all of them are also labelled in (a). The image was acquired with a sample bias voltage of V_S = +2.50 V and a tunnel current of I_T = 0.12 nA.

In the first approach we used a standard MMC method with periodic boundary conditions. The simulation slabs were built by using 9 layers of 1 1 0 atoms of Cu. While the last 2 bottom Cu layers were frozen to simulate the bulk, all the remaining atoms in the sample were allowed to move. Along the simulation, on each MC step all mobile atoms are randomly displaced by a fraction of the constant lattice and the energy of the resulting configuration is calculated. This configuration is accepted or rejected following the Metropolis criteria, i.e. if the energy decreases the new configuration is automatically accepted, if not, the decision depends on the comparison of the Boltzmann factor $P_i = \exp(\Delta E/kT)$, where ΔE is the energy increment, with a random number given by the calculation. In the past, this kind of MC simulation allowed us to understand the effect of surfactants on Cu(1 1 1) surfaces [24] and the anomalous growth of Co on Cu(1 1 1) [25].

In this MC method we employed realistic potentials that include long-ranged many-body Al–Al, Cu–Cu and Al–Cu interactions based on the second-moment approximation of the tight-binding scheme (TB-SMA) for the electronic structure description [26, 27]. The Born–Mayer pair and classic 6–12 Lennard–Jones potentials are used to describe the F–F, Cu–F and Al–F interactions. In addition, the ionic pairs are augmented with the Coulomb interaction [28].

As we said above, the second MC approach is based in the (LDA-MC) [29, 30] approach. This is the simplest model we can perform: an isolated atom lands on a square matrix and moves over it without limitation, i.e. the diffusion path is infinite and it moves until it reaches a nucleating center. After the nucleation occurs, another ad-atom is added to the simulation, i.e. only one atom moves at a time. We can vary several conditions, for instance the nucleation environment imposing the requirement of one, two or three neighbours, the maximum number in a square lattice. Although this is a quite simple model, we have successfully applied it to observe the fractal mode growth, including changes in the perimeter versus island size evolution slope, and shadowing effects in AlF_3 on Cu(1 0 0) [19, 20]. In this work we use this approach to study the effect of different step-edge properties, i.e. nucleating, inert step-edges and repulsive ones.

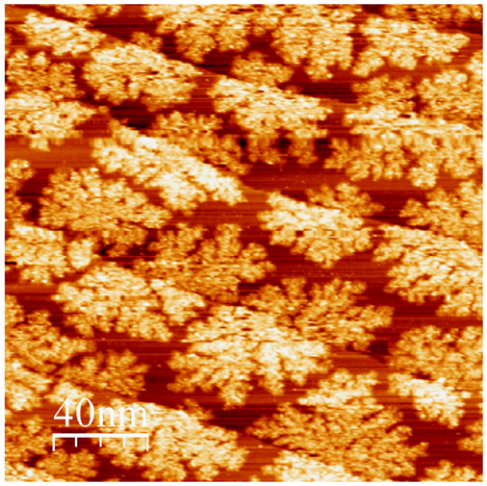

Figure 2. (a) STM image (200 nm × 200 nm) recorded after the deposition of 0.70 ML of AlF_3 on Cu(1 1 1). The image was acquired at V_S = +2.30 V and I_T = 0.10 nA.

3. Results and discussion

3.1. STM results

In order to study the growth of AlF_3 on Cu(1 1 1) at room temperature, we performed STM measurements at two different coverages: medium and saturation. In figure 1(a), we show a STM image of the surface after the deposition of 0.40 ML

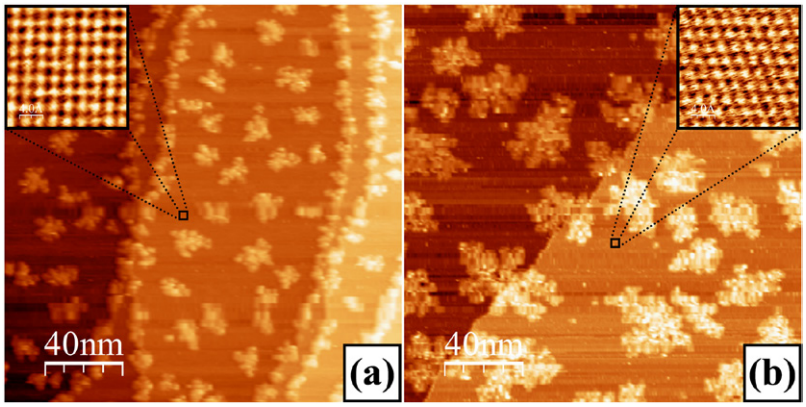

Figure 3. STM images (200 nm × 200 nm) recorded after the deposition of 0.30 and 0.40 ML of AlF_3 on (a) Cu(1 0 0) and (b) Cu(1 1 1), respectively. The images were acquired at $V_S = +2.50$ V and $I_T = 0.10$–0.12 nA. Insets: STM images (2 nm × 2 nm) recorded between the AlF_3 islands displaying the atomic resolution of the square and hexagonal structures of Cu(1 0 0) and Cu(1 1 1), respectively, with the following tunnelling conditions: (a) $V_S = -0.25$ V, $I_T = 1.0$ nA and (b) $V_S = +0.65$ V, $I_T = 2.5$ nA.

of AlF_3. At this coverage we observe a fractal islands growth similar to the case of AlF_3 on a Cu(1 0 0) surface. The density of islands on the terraces is about 1.0×10^{11} islands cm^{-2}, the average distance between first-neighbour islands is 25.0 nm, and their heights are in the range between 0.25 and 0.30 nm, i.e. one ML high (figure 1(b)). Looking at the right side of the image, another important issue can be pointed out: for narrow terraces, of about 30–40 nm, the probability to nucleate an island on them is practically zero, and a pseudo-step-flow regime is observed, as effectively occurs in step-edge bunched regions (not shown here) with terraces less than ~40.0 nm wide. This is clearly observed in the middle terrace (the one between the two step-edges) of the STM image shown in figure 1(a), and also in a higher density step-edged surface, at an almost saturation AlF_3 coverage (0.70 ML), as shown in figure 2. In both situations the STM images exhibit an important number of partially decorated step-edges without the formation of islands in the center of terraces, suggesting a diffusion length similar to or larger than the average distance between terrace islands.

In the middle scan profile of figure 1(b) we show that the apparent height of the AlF_3 islands is about 0.25–0.30 nm, as we have already stated above and elsewhere [19]. The difference between the islands and the Cu step-edges (~0.21 nm) heights allows us to identify if nucleation occurs either at the lower or upper side of a step-edge. The image shows islands nucleated on both sides of the step-edges (labelled 3) as confirmed by the bottom scan profile of figure 1(b).

It is remarkable that even with diffusion lengths clearly larger than the terraces width, step-edges are not fully decorated with AlF_3 molecules. Additionally, the behaviour of the nucleation at both sides of the step-edges is very different to the well-known case of metal-on-metal growth, on which nucleation sites are restricted to ascending step-edges, just due to the increased number of neighbours that increases the bonding energy [31]. Or even in some insulator-on-metal growth systems, like those reported by Farías *et al* [6] on the growth of LiF on Ag(1 1 1) at low temperatures (77 K) or Moreno-López *et al* [19] studying the AlF_3 on Cu(1 0 0) growth at room temperature, where both sides of the step-edges act as nucleation centers. The absence of step-edge decoration is associated with a diffusion path length smaller than the terrace size that leads to island nucleation. As we showed above for narrow terraces this is not the current case, i.e. we have an apparent contradictory result: on one side we have no island nucleation over these terraces and at the same time step-edges are not decorated. This effect leads us to think that a particular step-edge property is governing the growing process.

From the results depicted in figures 1(a) and 2, we conclude that not only AlF_3 molecules do not decorate step-edges, even when they have diffusion paths large enough to do so, but also nucleation of AlF_3 islands on Cu(1 1 1) proceeds in a symmetrical way at step-edges, i.e. the nucleation probability is almost the same for molecules approaching a step-edge from the upper or lower terraces. Although, nucleation at the step-edge upper terraces has been experimentally observed [6, 19, 25], they are exceptional cases, always founded in particular mechanisms. In the case of AlF_3 on Cu(1 1 1), we have all four possible situations at work: (i) preferential nucleation at the lower step-edge side (like in metal-on-metal growth) [32–35], (ii) preferential nucleation located at the upper step-edge side, (iii) nucleation at both sides of the step-edges and (iv) zones free of molecules at them. In figure 1(a), we observe that the islands size and their density is the same, independently if their location is at step-edges or in the middle of a terrace. This fact points out that islands not only grow at similar rates, but also with the same nucleation origin, i.e. no differences can be detected from either a critical nucleus at terraces or step-edges. So, as a conclusion we can state that step-edges are not acting as nucleation sources as a whole.

If we compare the present experimental results of AlF_3 growing on Cu(1 1 1) with those obtained on Cu(1 0 0) [19], we conclude that the growth of AlF_3 sub-monolayers on both faces show more differences than similarities. Although, for both cases we observe the formation of fractal islands of the same height and very corrugated surfaces, similarities end at this point. As Cu(1 1 1) is a more compact surface, we expect a smaller diffusion barrier, with a larger diffusion path on this surface, as indeed occurs, i.e. the islands are remarkably larger on this face than for Cu(1 0 0) (figure 3).

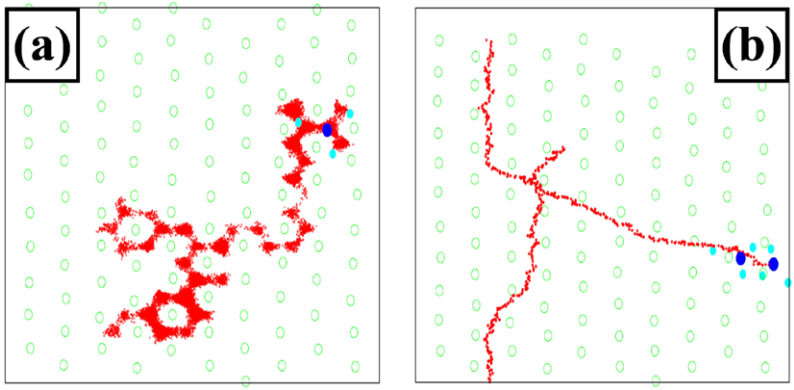

Figure 4. Different paths given by MMC simulations for an (a) isolated molecule (2×10^6 MC steps) and a (b) reconstructed bi-molecule (5×10^4 MC steps) over a Cu(1 1 1) surface. Blue circles represent Al atoms, light blue F atoms and green Cu atoms, the red lines represent the trajectories or positions of the Al atoms obtained along simulations.

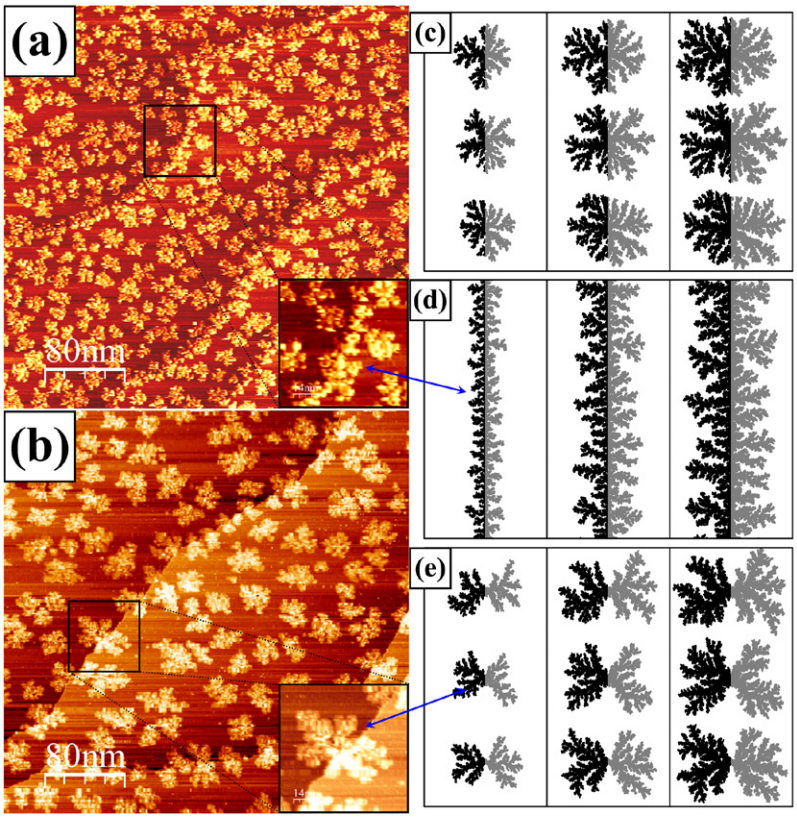

Figure 5. Left column: STM images (400 nm × 400 nm) of Cu surfaces covered with AlF_3 molecules. (a) 0.5 ML of AlF_3 on Cu(1 0 0), (b) 0.4 ML of AlF_3 on Cu(1 1 1). Insets: STM images (70 nm × 70 nm) which show the shape of the step-edges islands. Right column: LDA-MC simulation snapshots. Each snapshot corresponds to a simulation which starts from three nucleation sites resembling (c) only a terrace and an imaginary line simulating a (d) Cu(1 0 0) and (e) Cu(1 1 1) step-edges considered as nucleating and reflecting, respectively. The coverage increases from left to right, taking values of 0.1, 0.2 and 0.3 ML. The images were acquired at $V_S = +2.50$ V and $I_T = 0.12$–0.15 nA.

In figure 3, we show two STM images recorded after deposition of 0.30 and 0.40 ML of AlF_3 on Cu(1 0 0) and Cu(1 1 1), respectively. For 0.40 ML AlF_3 coverage on Cu(1 1 1) (figure 3(b)), the average distance between islands is 25 nm and the surface island density is 1.0×10^{11} islands cm^{-2}, while for 0.25 ML of AlF_3 and beyond that coverage on Cu(1 0 0) (0.30 ML of AlF_3 in figure 3(a)), the average distance between islands and surface island density have constant values of 17 nm and 1.5×10^{11} islands cm^{-2}, respectively. Clearly, these results show that the surface diffusion path of AlF_3 on Cu(1 1 1) is larger than in the other face.

However, critical unexpected differences appear as soon as we take a look at the behaviour around step-edges. While on Cu(1 0 0) they are completely decorated, on Cu(1 1 1) the step-edges show long non-covered zones, even at coverages as high as 0.70 ML (see figure 2), and for a substantially larger diffusion path as we already pointed out. Since a larger diffusion path implies an easier way to reach step-edges, the

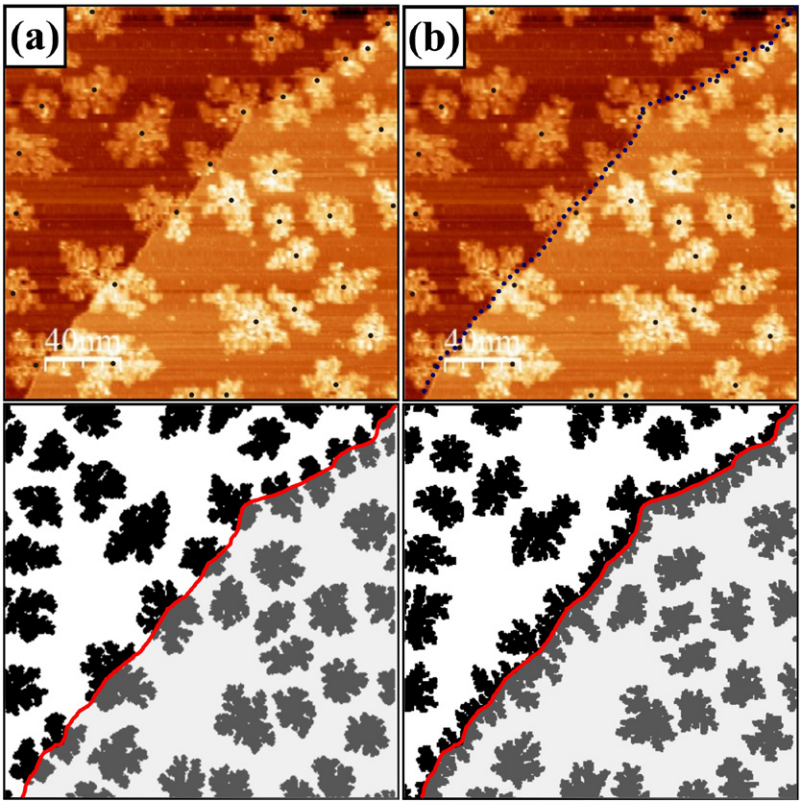

Figure 6. Top: STM images (200 nm × 200 nm) of a Cu(1 1 1) surface covered with 0.40 ML of AlF_3 with nucleation centers marked with black dots (a) only on top of the islands and (b) over the step-edge as well. Bottom: simulated LDA-MC surface images, using as initial nucleation centers the points marked in (a) and (b). As a guide for the eye, in both LDA-MC snapshots we added a red line which represents the experimental step-edge separating the lower (left) and upper (right) terraces. In the right LDA-MC snapshot a nucleating step-edge was simulated by locating an almost continuous line of nucleation centers at the step-edge as seen in (b). The image was acquired at $V_S = 2.50$ V and $I_T = 0.12$ nA.

explanation of not fully decorated step-edges on the Cu(1 1 1) face requires a different reasoning. With the aim of understanding some of these questions we performed the MMC and LDA-MC simulations.

3.2. Metropolis Monte Carlo simulations

The MMC calculation results for Cu(1 1 1) show similarities with those of Cu(1 0 0) as far as isolated molecules and reconstructed bi-molecules surface diffusion is concerned [21]. In figure 4, we show the trajectories and visited sites (steps) of an isolated molecule and a reconstructed bi-molecule over a Cu(1 1 1) surface at room temperature. While the first ones show an isotropic diffusion by hopping (see figure 4(a)), the reconstructed bi-molecules do not, diffusing over the surface along favoured directions (see figure 4(b)) and showing as well an important change in the diffusion length (almost two orders of magnitude in the number of MMC steps) with respect to the one corresponding to isolated molecules, similarly to Cu(1 0 0) [21]. This movement along the surface channels, with a significant change in the diffusion length, produces an important difference between the growth mode on both surfaces, due to the privileged directions for Cu(1 1 1) being three, against two for Cu(1 0 0).

When AlF_3 molecules reach the Cu(1 1 1) surface they diffuse isotropically over it, instead when the reconstructed bi-molecules arrive or are formed, they move along the three main directions of symmetry of the crystal hexagonal lattice. Similar results have been observed for Cu(1 0 0), but in that case the movement was only along the two main directions of symmetry of the crystal square lattice [21]. Thus, as for Cu(1 1 1) the favoured directions are three, exhibiting the reconstructed bi-molecules a very high mobility along them, and for Cu(1 0 0) only two, once the island critic cores are formed, the probability of receiving new contributions is 50% higher, justifying the larger size and lower island surface density observed during the experiments.

3.3. LDA Monte Carlo simulations

In figure 5, we compare STM images taken after the deposition of 0.5 and 0.4 ML of AlF_3 on Cu(1 0 0) and Cu(1 1 1), respectively, with some snapshots of LDA-MC simulations that may help to understand the different growth morphologies at step-edges.

From the STM images shown in figures 5(a) and (b), it is clear that while for Cu(1 0 0) the AlF_3 islands completely decorate step-edges, on Cu(1 1 1) these are only partially covered by AlF_3 islands. At the same time for both surfaces, the nucleation of AlF_3 islands at step-edges proceeds in a rather symmetrical way, i.e. the nucleation probability is almost the same for AlF_3 molecules approaching a step-edge from the

upper or lower terraces. However, the shape of the nucleated step-edge islands looks very different. Besides, on both surfaces they show fractal shapes, for Cu(1 1 1) the islands have a '*butterfly*' aspect not seen on the Cu(1 0 0) surface (see insets). All these experimental facts can be understood on the basis of peculiar different properties of both kinds of step-edges, which can be simulated within the simple framework given by the LDA-MC model.

The results are shown on the right column of figure 5. There we show simulations of the growth of AlF_3 islands that start from three nucleation sites located along an imaginary vertical line. In figure 5(c), this line has not a particular meaning and the simulation only resembles the growth of islands on a terrace. On the other hand, in figures 5(d) and (e) it simulates a vertical step-edge with a particular characteristic we attribute to a Cu(1 0 0) or Cu(1 1 1) surface, respectively. The snapshots (3 for each case, the terrace, Cu(1 0 0) and Cu(1 1 1)) correspond to different coverages increasing from left to right, taking values of 0.1, 0.2 and 0.3 ML. While for Cu(1 0 0) the step-edge is assumed to be nucleating (figure 5(d)), i.e. every molecule arriving to the step-edge stays there, for Cu(1 1 1) it is considered to be non-nucleating (figure 5(c)) or repulsive (figure 5(e)), and i.e. a molecule that arrives to the step-edge is reflected. The similarities between the measured growth morphologies and LDA-MC simulations for each particular case are remarkable.

In figure 6, we show another LDA-MC simulation where we tried to describe a situation closer to an experimental scenario in which several islands coexist on terraces and step-edges, growing simultaneously, and competing to capture adsorbed molecules. In analysing LDA-MC (and Metropolis MC) results one needs to keep in mind that we are using periodical conditions. Within these conditions, molecules leaving the frame through the upper or right side return into the scenario again at the lower or left side, respectively. Thus, when an island nucleates close to a border, the molecules see this island from both sides of the frame, giving a sense of symmetry that is not real. This problem appears due to the fact that we need to work with finite samples. The approximation is better, the larger the simulated terraces are. Since our LDA-MC simulation evolution needs an initial distribution of nucleation centers to begin [19], we got them from the central points of the islands observed in the experimental STM image. These centers are represented by black dots in the STM image shown on figure 6(a). The agreement between the experimental STM image and LDA-MC simulation, shown in the bottom left panel, is significant. The simulation resembles the entire main experimental features of the AlF_3 film, and emphasizes the reflecting nature of step-edges in the Cu(1 1 1) surface. On the other hand, in the bottom right panel, we show a LDA-MC simulation where we added to the nucleation centers used before an almost continuous line of nucleation centers located at the step-edge (see the STM image of figure 6(b)). In this situation, the simulation gives the usual distribution of smaller islands at the step-edge, a characteristic of the AlF_3 growth on the Cu(1 0 0) surface as seen in figures 3(a) and 5(a) (see the inset as well) [19], and a signature of the nucleating nature of the step-edges of this surface.

4. Conclusion

In this work, we studied the AlF_3 thin film growth on Cu(1 1 1) at room temperature by means of STM, LDA and MMC simulations, comparing the results with previous ones obtained on Cu(1 0 0). The growth of AlF_3 sub-monolayers on Cu(1 1 1) shows more differences than similarities compared with the deposition on Cu(1 0 0). In both cases, we observe the formation of fractal islands, with very corrugated surfaces and similar heights, 0.25–0.30 nm. The step-edges on Cu(1 1 1) are not completely decorated as they are in the case of Cu(1 0 0), even at large coverages (>0.7 ML). The islands are larger in size (this gives longer average distances) and consequently its density is smaller. These experimental results can be understood by means of LDA and MMC calculations. On Cu(1 1 1), when the reconstructed bi-molecules are formed, they move along three privileged directions instead of two observed for Cu(1 0 0), the potentiality of receiving new contributions is 50% higher, justifying the larger sizes and smaller surface density of the islands observed in the experiments. While the characteristic of the (1 0 0) copper face step-edges appears to be nucleating, the (1 1 1) copper face step-edges seem to be of a repulsive nature.

Acknowledgments

This work was financially supported by CONICET, ANPCyT and UNL, through projects PIP 2012–2014 Grant No 577; PICT 2010 Grant No 0294 and PICT 2013 Grant No 0164; and CAI+D 2011 Grant No 501 201101 00283 LI (A) and PACT 2011 Grant No 84; respectively. The authors acknowledge the support and kind contributions of Dr J C Moreno-López to the discussion of this work.

References

[1] Zhang Z and Lagally M G 1997 *Science* **276** 377
[2] Sun X, Felicissimo M P, Rudolf P and Silly F 2008 *Nanotechnology* **19** 495307
[3] Hirjibehedin C F, Lutz C P and Heinrich A J 2006 *Science* **312** 1021
[4] Ramoino L, Von Arx M, Shintke S, Baratoff A, Güntherodt H-J and Jung T A 2006 *Chem. Phys. Lett.* **417** 22
[5] Calleja F, Hinarejos J J, Vázquez de Parga A L, Suturin S M, Sokolov N S and Miranda R 2005 *Surf. Sci.* **582** 14
[6] Farías D, Braun K-F, Fölsch S, Meyer G and Rieder K H 2000 *Surf. Sci. Lett.* **470** L93
[7] Bertrams Th and Neddermeyer H 1996 *J. Vac. Sci. Technol.* B **14** 1141
[8] Fölsch S, Helms A, Zöphel S, Repp J, Meyer G and Rieder K H 2000 *Phys. Rev. Lett.* **84** 123
[9] Muray A, Scheinfein M, Isaacson M and Adesida I 1985 *J. Vac. Sci. Technol.* B **3** 367
[10] Chen G S 1999 *J. Vac. Sci. Technol.* A **17** 403
[11] Langheinrich W, Spangenberg B and Beneking H 1992 *J. Vac. Sci. Technol.* B **10** 2868
[12] Watanabe H, Fujita J, Ochiai Y, Matsui S and Ichikawa M 1995 *Japan. J. Appl. Phys.* **34** 6950
[13] Vergara L I, Vidal R A, Ferrón J, Sánchez E A and Grizzi O 2001 *Surf. Sci.* **482-5** 854

[14] Vergara L I, Vidal R A and Ferrón J 2004 *Appl. Surf. Sci.* **229** 301
[15] Muray A, Isaacson M and Adesida I 1984 *Appl. Phys. Lett.* **45** 589
[16] Nikolaichik V I 1993 *Phil. Mag.* A **68** 227
[17] Chen G S and Humphreys C J 1997 *J. Vac. Sci. Technol.* B **15** 1954
[18] Sánchez E A, Otero G, Tognalli N, Grizzi O and Ponce V H 2003 *Nucl. Instrum. Methods Phys. Res.* B **203** 41
[19] Moreno-López J C, Vidal R A, Passeggi M C G Jr and Ferrón J 2010 *Phys. Rev.* B **81** 075420
[20] Moreno-López J C, Passeggi M C G Jr, Ruano G, Vidal R A and Ferrón J 2010 *Phys. Status Solidi.* C **7** 2712
[21] Gómez L, Martín V, Garcés J and Ferrón J 2014 *J. Phys. D: Appl. Phys.* **47** 495305
[22] Horcas I, Fernández R, Gómez-Rodríguez J M, Colchero J, Gómez-Herrero J and Baro A M 2007 *Rev. Sci. Instrum.* **78** 013705
[23] Binder K 1992 *Monte Carlo Method in Condensed Matter Physics* vol 71 (Berlin: Springer)
[24] Camarero J, Ferrón J, Cros V, Gómez L, Vázquez de Parga A L, Gallego J M, Prieto J E, de Miguel J J and Miranda R 1998 *Phys. Rev. Lett.* **81** 850
[25] Gómez L, Slutzky C, Ferrón J, de la Figuera J, Camarero J, Vázquez de Parga A L, de Miguel J J and Miranda R 2000 *Phys. Rev. Lett.* **84** 4397
[26] Tománek D, Mukherjee S and Bennemann K H 1983 *Phys. Rev.* B **28** 665
Ducastelle F (ed M Meyer and V Pontikis) 1991 *Computer Simulation in Materials Science* (*NATO Advanced Study Institute, Series E, Applied Physics* vol 205) (Dordrecht: Kluwer Academic) p 233
[27] Mottet C, Tréglia G and Legrand B 1993 *Phys. Rev.* B **46** 16018
Cleri F and Rosato V 1993 *Phys. Rev.* B **48** 22
[28] Abrahamson A A 1969 *Phys. Rev.* **178** 76
Chaudhuri S, Chupas P J, Wilson M, Madden P and Grey C P 2004 *J. Phys. Chem.* B **108** 3437
Castiglione M J, Wilson M and Madden P A 1999 *Phys. Chem. Chem. Phys.* **1** 165
Inoue H, Soga K and Makishima A 2003 *J. Non-Cryst. Solids* **331** 58
[29] Witten T A Jr and Sander L M 1981 *Phys. Rev. Lett.* **47** 1400
[30] Meakin P 1983 *Phys. Rev.* A **27** 1495
[31] Nùrskov J K 1990 *Rep. Prog. Phys.* **53** 1253
[32] Hwang R Q, Schröder J, Günther C and Behm R J 1991 *Phys. Rev. Lett.* **67** 3279
[33] Brune H, Romainczyk C, Röder H and Kern K 1994 *Nature* **369** 469
[34] Kellogg G L 1994 *Surf. Sci. Rep.* **21** 1
[35] de Miguel J J 1997 *Surf. Rev. Lett.* **4** 353